ELSEVIER

Journal of Alloys and Compounds 391 (2005) 194–197

Journal of ALLOYS AND COMPOUNDS

www.elsevier.com/locate/jallcom

Effects of partial substitution of Co by Ni on the high-temperature thermoelectric properties of TiCoSb-based half-Heusler compounds

Min Zhou, Chude Feng, Lidong Chen*, Xiangyang Huang

State Key Laboratory of High Performance Ceramics and Superfine Microstructure, Shanghai Institute of Ceramics, Chinese Academy of Sciences, Shanghai 200050, PR China

Received 28 May 2004; accepted 28 July 2004
Available online 28 October 2004

Abstract

TiCoSb-based half-Heusler compounds were prepared by solid-state reaction and their thermoelectric properties were studied. The un-doped TiCoSb compound shows n-type conduction and demonstrates high Seebeck coefficient at high temperatures. The partial substitution of Co by Ni caused great increase in electron concentration and electrical conductivity, while the Seebeck coefficient and the thermal conductivity showed little change when Ni content (x) is below 5%. A maximum power factor of 16 $\mu W/K^2$ cm and a maximum dimensionless figure of merit (ZT) of 0.27 have been obtained for the composition of $TiCo_{0.95}Ni_{0.05}Sb$ at 900 K.

PACS: 72.20.Pa; 72.15.Jf; 72.80.−r

Keywords: Half-Heusler compounds; Seebeck coefficient; Electrical conductivity; Thermal conductivity

1. Introduction

Thermoelectric materials have attracted a renewed interest in recent years. The performance of a thermoelectric material is usually evaluated by the dimensionless figure of merit $ZT = S^2\sigma T/\kappa$, where S, σ, T and κ are Seebeck coefficient, electrical conductivity, absolute temperature and thermal conductivity, respectively. A good thermoelectric material should possess high Seebeck coefficient, high electrical conductivity and low thermal conductivity.

The half-Heusler compounds crystallize in the MgAgAs-type structure, which is built from three interpenetrating face-centered-cubic (fcc) sub-lattices of equal unit cell size. Two of the fcc sub-lattices, Ti and Sb sub-lattices in the case of TiCoSb, for example, combine to form a rock-salt sub-structure. The third fcc sub-lattice, Co, is displaced along the body diagonal of the rock-salt substructure by one-fourth of the unit cell (Fig. 1). Band structure studies of half-Heusler compounds gave the magnitude of energy gap as 0.1–0.9 eV and suggested a high Seebeck coefficient S that arises as a consequence of the narrow band with heavy carrier mass [1–6]. The high Seebeck coefficient and moderately large electrical conductivity make them attractive candidates for thermoelectric applications. Recent interest in half-Heusler compounds is just due to their promising thermoelectric properties.

ZrNiSn-based half-Heusler compounds have been extensively investigated for their thermoelectric properties in the past several years [7–11]. These compounds were reported to exhibit semi-conducting properties with high Seebeck coefficients in the order of a hundred μV/K. Doping with less than 1 at.% Sb on the Sn site results in a great increase of electrical conductivity without significant reduction of Seebeck coefficient and leads to large power factors ($S^2\sigma$) [12]. The thermal conductivity of ZrNiSn-based half-Heusler was reported to be depressed by alloying Hf on the Zr site and alloying Pd on the Ni site. Therefore the ZT value was greatly improved by the combination of Sb-doping and partial substitution of Zr or Ni by Hf or Pd [13].

* Corresponding author. Tel.: +86 21 52412520.
E-mail address: cld@mail.sic.ac.cn (L. Chen).

0925-8388/$ – see front matter © 2004 Elsevier B.V. All rights reserved.
doi:10.1016/j.jallcom.2004.07.074

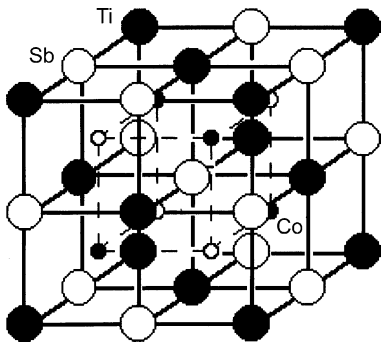

Fig. 1. The crystalline structure of TiCoSb compound. The small circles represent vacancies.

TiCoSb compound with a wider energy gap of 0.95 eV is a new family of half-Heusler compounds exhibiting semiconducting characters [1]. Both the Seebeck coefficient and electrical conductivity of TiCoSb compound at room temperature are comparable to those of ZrNiSn compound [8,12,14–17]. It was also shown by the studies on the transport of TiCoSb-based half-Heusler compounds at low temperature (below room temperature) that moderate doping of Nb, Ta, Ni or Pt results in the increase of power factor [15]. However, there have been no reports on the high temperature thermoelectric properties so far. In the present study, preparation and high temperature thermoelectric properties of TiCoSb-based half-Heusler are reported, especially the effect of Co substitution by Ni on the thermoelectric properties are investigated.

2. Experimental procedure

$TiCo_{1-x}Ni_xSb$ ($x = 0, 0.01, 0.025, 0.05, 0.1$) samples were prepared by a solid-state reaction method. The highly pure constituents of Ti (99.5%, powder), Co (99.99%, powder), Sb (99.9999%, powder), Ni (99.996%, powder) were used as starting materials. The mixed powder was pressed into pellets and then heated to 1173 K in a carbon crucible under a flowing argon atmosphere for 120 h. The reacted materials were milled into fine powder and consolidated by a spark plasma sintering technique (Sumitomo Coal Mining, SPS-2040) at 1123 K for 6 min.

The phase composition of the samples was examined by X-ray diffraction (XRD) analysis with Rigaku RINT2000 (Cu Kα radiation). The carrier concentration n was measured by the bar method using a Hall measurement system (Accent 5500). The electrical conductivity (σ) was measured in the temperature range from 300 to 900 K, using a standard dc technique in a four terminal arrangement with bare gold wires being glued to the samples by conducting silver epoxy. The thermoelectromotive force (ΔE) was measured at five different temperature gradients ($0 \leq \Delta T \leq 5$ K) for a given temperature, and the Seebeck coefficient (α) was obtained from the slope of ΔE versus ΔT plot. The thermal conductivity (κ) was calculated from the values of density, specific heat capacity and thermal diffusivity. And the thermal diffusivity was measured by a laser flash technique (NETZSCH LFA427) in Ar atmosphere over the temperature range from 300 K to 900 K.

3. Results and discussion

Fig. 2 shows typical XRD patterns of the $TiCo_{1-x}Ni_xSb$ samples. XRD analysis confirmed that all the samples were crystallized in the single-phase with MgAgAs crystalline structure. A lattice parameter of 0.5882 nm for the un-doped sample was obtained. This value is consistent with the data ($a = 0.5884$ nm) reported by Webster and Ziebeck [18]. The lattice parameters of $TiCo_{1-x}Ni_xSb$ ($0 < x \leq 0.1$) only showed a little change after doping Ni on Co site, for example, the lattice parameter of $TiCo_{0.90}Ni_{0.10}Sb$ was measured as 0.5880 nm, because the atomic radius of Ni (0.1620 nm) is very close to that of Co (0.1670 nm).

Fig. 3 displays the temperature dependence of electrical conductivity for $TiCo_{1-x}Ni_xSb$. The electrical conductivity of the un-doped TiCoSb compound was in the order of $10^3\ \Omega^{-1}\ m^{-1}$ and increased with increasing Ni content. The σ values increased by more than one order of magnitude from appropriately $4 \times 10^3\ \Omega^{-1}\ m^{-1}$ for TiCoSb to as high

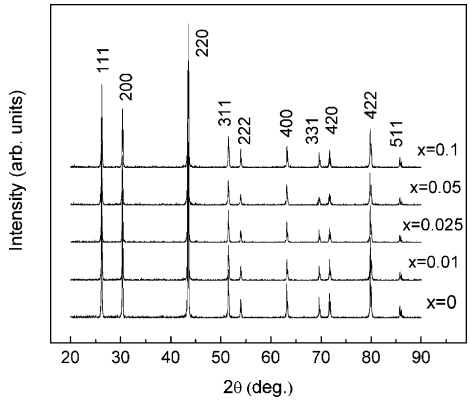

Fig. 2. The X-ray diffraction pattern of $TiCo_{1-x}Ni_xSb$ samples.

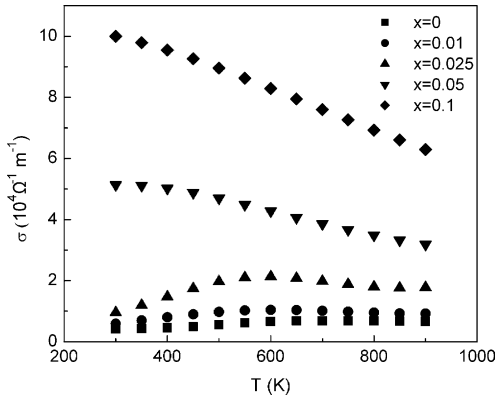

Fig. 3. Temperature dependence of the electrical conductivity for $TiCo_{1-x}Ni_xSb$ samples.

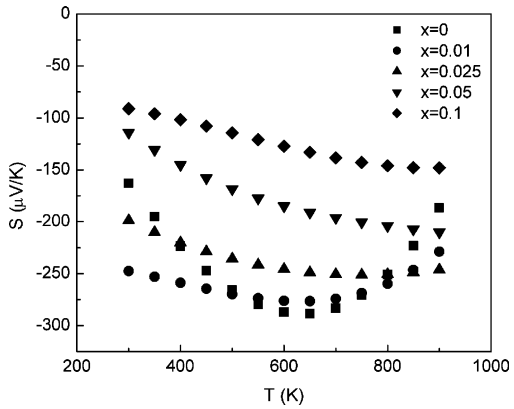

Fig. 4. Temperature dependence of the Seebeck coefficient for $TiCo_{1-x}Ni_xSb$ samples.

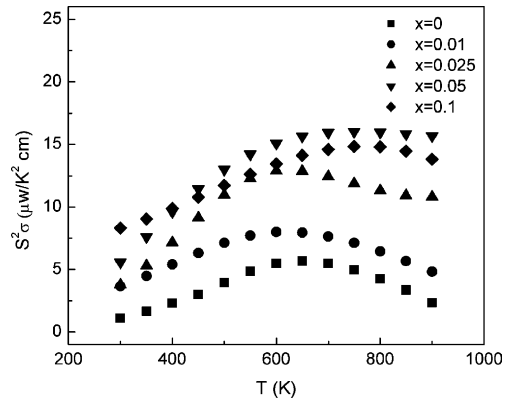

Fig. 5. Temperature dependence of the power factor for $TiCo_{1-x}Ni_xSb$ samples.

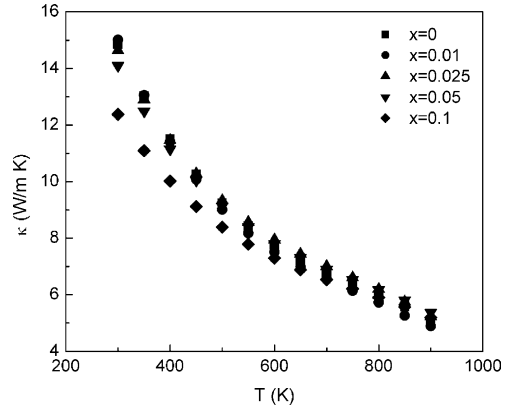

Fig. 6. Temperature dependence of the thermal conductivity for $TiCo_{1-x}Ni_xSb$ samples.

as $1 \times 10^5\ \Omega^{-1}\,m^{-1}$ for $TiCo_{0.9}Ni_{0.1}Sb$ at room temperature. The $TiCo_{1-x}Ni_xSb$ compounds exhibited semiconductor-to-semimetal (SC–SM) transition at 500∼650 K when Ni content (x) is less than 0.05, and the SC–SM transition temperature shifts to lower temperatures when Ni content increased. A further increase of Ni-doping content ($x \geq 0.05$), a metal-like behavior was observed over the measured temperature range. A similar change in σ is also reported in ZrNiSn-based half-Heusler compounds. In that system, the temperature dependence of σ changed from an activated behavior to a metal-like one after doping Sb on Sn site, which was considered to be due to the band overlap [7–9,12].

Fig. 4 shows the temperature dependence of Seebeck coefficient for $TiCo_{1-x}Ni_xSb$. The un-doped TiCoSb compound exhibited a relatively large negative Seebeck coefficient because of the heavy electron band mass. The absolute values of α ($|\alpha|$) decreased after doping Ni on Co site, which is consistent with the increase of σ. The changes of σ and α are considered to be contributed by the increase of electron concentration [8,12,13] (as shown in Table 1) after the partial substitution of Ni on Co site because Ni possesses one more covalent electron than Co. For the samples of $x < 0.05$, $|\alpha|$ values showed peaks at about 650 K. Below 650 K $|\alpha|$increases with increasing temperature, which indicates that the conduction may be dominated by extrinsic charge carriers excited from the impurity state. $|\alpha|$ values reached a maximum at about 650 K and then decreased with increasing temperature. This is considered to be due to the excitation of electron-hole pairs across the energy gap, because the opposing contributions to Seebeck coefficient from the two carriers reduce the observed $|\alpha|$. A similar behavior is also reported for ZrNiSn-based half-Heusler [11,12]. When Ni content (x) is more than 0.05, $|\alpha|$ increases monotonously with temperatures in the measured temperature range. This is consistent with the metal-like conducting behavior of $TiCo_{1-x}Ni_xSb$ ($x \geq 0.05$) observed in the temperature dependence of electrical conductivity shown in Fig. 3. The contribution of hole carriers to Seebeck coefficient is neglectable for a metal-like compound [19].

Fig. 5 shows the temperature dependence of power factors ($S^2\sigma$) for $TiCo_{1-x}Ni_xSb$. Power factors of the samples are observed to rapidly increase as Ni doping content increased. When Ni content (x) is 0.05, $S^2\sigma$ reaches a maximum value of 16 $\mu W/K^2$ cm at about 750 K. This value is around three-fold increase as compared to the un-doped TiCoSb sample.

Fig. 6 indicates the temperature dependence of thermal conductivity for $TiCo_{1-x}Ni_xSb$. Thermal conductivity showed little change after doping Ni on Co site. Thermal conductivity can be expressed by the sum of a phonon conduc-

Table 1
Carrier concentration n and the electrical conductivity σ of $TiCo_{1-x}Ni_xSb$ samples

Samples	TiCoSb	$TiCo_{0.99}Ni_{0.01}Sb$	$TiCo_{0.975}Ni_{0.025}Sb$	$TiCo_{0.95}Ni_{0.05}Sb$	$TiCo_{0.90}Ni_{0.10}Sb$
n (10^{19}/cm^3)	0.3	0.8	1.3	7.2	9.1
σ ($10^4\ \Omega^{-1}\,m^{-1}$)	0.42	0.60	0.96	5.14	10.00

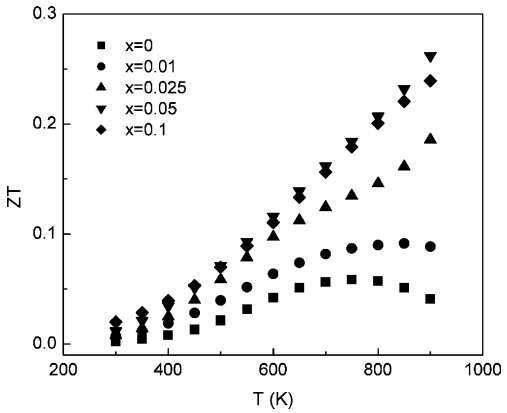

Fig. 7. Temperature dependence of the dimensionless figure of merit (ZT) for $TiCo_{1-x}Ni_xSb$ samples.

tion component and an electronic component as $\kappa = \kappa_l + \kappa_e$. κ_e can be estimated from Wiedemann–Franz's law as $\kappa_e = LT\sigma$, where L is the Lorenz number (2.45×10^{-8} V^2 K^{-2} for free electrons). For $TiCo_{1-x}Ni_xSb$ compounds, it is estimated that κ_e is between 0.03 and 0.38 W/m K for different compositions. Clearly, κ_e is only a small part of the total thermal conductivity. As a result, κ comes largely from the lattice component contribution (κ_l). The un-doped TiCoSb compound has a relatively high thermal conductivity of approximately 15 W/m K at room temperature. After doping Ni on Co site, the decrease of κ is not obvious because of the small levels of doping of Ni ($x \leq 0.1$) and the close proximity of Co and Ni in the periodic table, which results in unnoticeable mass-fluctuation scattering between Ni (atomic mass = 58.7) and Co (atomic mass = 58.9). Thermal conductivities of $TiCo_{1-x}Ni_xSb$ compounds decreased with temperature and reached about 5 W/m K at 900 K. The decrease of κ with temperature is mainly caused by the phonon–phonon scattering.

Fig. 7 shows ZT of all the samples in the temperature range of 300 to 900 K. The ZT values tend to increase with temperature due to the rapid decrease of thermal conductivity, in spite of a little decrease of power factor at high temperature ($T > 650$ K). Ni doping resulted in the increase of ZT value. A maximum value of 0.27 is obtained for the $TiCo_{0.95}Ni_{0.05}Sb$ sample at 900 K, which is nearly 7 times larger than the undoped TiCoSb compound.

4. Conclusion

An extensive investigation on the effect of Ni substituting in the half-Heusler compounds $TiCo_{1-x}Ni_xSb$ is presented through electrical conductivity, Seebeck coefficient and thermal conductivity as a function of temperature. These compounds show high negative Seebeck coefficients (−91 to −188 μV/K) and moderately large electrical conductivity. Ni doping improved the electrical transport property of these compounds. A moderate power factor of about 16 $\mu W/K^2$ cm has been observed in doped compounds of $TiCo_{0.95}Ni_{0.05}Sb$ at 750 K. The dimensionless figure of merit ZT is much enhanced by Ni doping on Co site and the maximum value of ZT (0.27) is obtained at 900 K for $TiCo_{0.95}Ni_{0.05}Sb$. The thermal conductivities of these compounds are between 12 and 15 W/m K at 300 K and still much higher than that of the state-of-the-art materials. It is expected to further improve the thermoelectric performance of $TiCo_{1-x}Ni_xSb$ system especially by depressing lattice thermal conductivity through introducing some extra phonon modes into this system.

Acknowledgment

This work was partially supported by the National High Technology Research and Development Program of China (863 Program) under Grant No. 2001AA323070 and National Natural Science Foundation of China under Grant No. 50325208.

References

[1] J. Tobola, J. Pierre, S. Kaprayk, R.V. Skolozdra, M.A. Kouacou, J. Phys.: Condens. Matter 10 (1998) 1013.
[2] F.G. Aliev, N.B. Brandt, V.V. Moshchalkov, V.V. Kozyrkov, R.V. Skolozdra, A.I. Belogorokhov, Phys. B: Condens. Matter 75 (1989) 167.
[3] F.G. Aliev, Physica B 171 (1991) 199.
[4] R. Kuentzler, R. Clad, G. Schmerber, Y. Dossmann, J. Magn. Magn. Mater. 104–107 (1992) 1976.
[5] C.S. Lue, Y.K. Kuo, Phys. Rev. B 66 (2002) 85121.
[6] B.A. Cook, J.L. Harringa, Z.S. Tan, W.A. Jesser, Proceedings of the 15th International Conference on Thermoelectrics, 1996, p. 122.
[7] C. Uher, J. Yang, S. Hu, D.T. Morelli, G.P. Meisner, Phys. Rev. B 59 (1999) 8615.
[8] H. Hohl, A.P. Ramirez, C. Goldmann, G. Ernst, B. Wolfing, E. Brcher, J. Phys.: Condens. Matter 11 (1999) 1697.
[9] S.J. Poon, T.M. Tritt, Y. Xia, S. Battacharya, V. Ponnambalam, A.L. Pope, R.T. Littleton, V.M. Browning, Proceedings of the 18th International Conference on Thermoelectrics, 1999, p. 45.
[10] J. Pierre, R.V. Skolozdra, J. Tobola, S. Kaprzyk, C. Hordequin, M.A. Kouacou, I. Karla, R. Currat, J. Alloys Comp. 262/263 (1997) 101.
[11] V. Ponnambalam, A.L. Pope, S. Bhattacharya, Y. Xia, S.J. Poon, T.M. Tritt, Proceedings of the 18th International Conference on Thermoelectrics, 1999, p. 340.
[12] S. Bhattacharya, A.L. Pope, R.T. Littleton IV, T.M. Tritt, V. Ponnambalam, Y. Xia, S.J. Poon, Appl. Phys. Lett. 77 (2000) 2476.
[13] Q. Shen, L.D. Chen, T. Goto, T. Hirai, J. Yang, G.P. Meisner, C. Uher, Appl. Phys. Lett. 79 (2001) 4165.
[14] Y. Xia, S. Bhattacharya, V. Ponnambalam, A.L. Pope, S.J. Poon, T.M. Tritt, J. Appl. Phys. 88 (2000) 1952.
[15] Y. Xia, V. Ponnambalam, S. Bhattacharya, A.L. Pope, S.J. Poon, T.M. Tritt, J. Phys.: Condens. Matter 13 (2001) 77.
[16] C. Uher, J. Yang, G.P. Meisner, Proceedings of the 18th International Conference on Thermoelectrics IEEE catalog No. 99TH8407, IEEE, Piscataway, NJ, 1999, p. 56.
[17] Y. Stadnyk, Y. Gorelenko, A. Tkachuk, A. Goryn, V. Darydov, D. Bodak, J. Alloys Comp. 329 (2001) 37.
[18] P. Webster, Ziebeck, J. Phys. Chem. Solids 34 (1973) 1647.
[19] N. Cusack, P. Kendall, Proc. Phys. Soc. London 72 (1958) 898.